Chapter 6

Topology of Flow Shapes

Summary. In this chapter we analyze the topology of flow shapes, i.e., the underlying spaces of sub-complexes of the flow complex. On the basis of the algorithm of the previous chapter, we establish a topological similarity between flow shapes and the nerve of a corresponding ball set, namely homotopy equivalence.

6.1 Introduction

Flow shapes are obtained from the flow complex of a set of points by restricting the influence of the points to a maximum distance α, i.e., to a ball of radius $\sqrt{\alpha}$ since we are considering the power distance. Varying the distance α yields a filtration of the flow complex, i.e., a family of nested sub-complexes. A flow shape is the topological space underlying a sub-complex. In this chapter the recursive structure of the stable manifolds captured by the algorithm in the previous chapter is used to analyze topological properties of flow shapes.

Flow shapes are shape constructors, i.e., they transform finite point sets into continuous shapes. The choice of the influence distance α for the points allows multi-scale modeling which turns out to be useful in detecting features at different scales. Due to their practical importance in geometric modeling, various shape constructors have been proposed recently. Understanding the relationship among them leads to new insights potentially helpful in applications. An overview of various shape constructors and their relation is given by Carlsson and de Silva [31].

We place flow shapes in relation to these shape constructors by proving that the flow shape for a distance α is homotopy equivalent to the union of balls of radius $\sqrt{\alpha}$. A natural representation of the topology of the union of balls is the Čech complex of the balls. The Čech complex is the nerve of the ball set, i.e., it is the simplicial complex with a vertex for every ball and a simplex for every subset of balls with non-empty intersection. By the Čech theorem the Čech complex is homotopy equivalent to the union of these balls and therefore by the result of this chapter to the corresponding flow shape.

The Čech complex is inefficient in representing the underlying topology in the sense that a large number of simplices (and in particular higher-dimensional

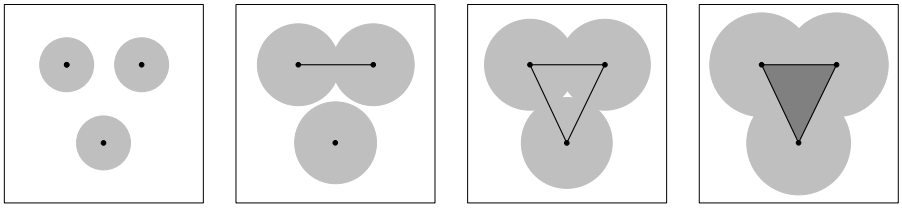

(a) (b) (c) (d)

Figure 6.1: Filtration of a flow complex.

simplices) might be used to represent a simple topological space. The α-shape complex [62] is a simplicial complex (with a scale parameter α) that has the same homotopy type as the Čech complex [58] but is embedded in $\mathbb{R}^d$ and has many fewer simplices. When varying α, the Čech complex and therefore also the α-shape complex and the flow shapes change their homotopy type only at discrete critical levels. An illustration of these complexes for different values of α is given in Figure 6.2 in Section 6.3. In contrast to the other two complexes, the geometry of the flow shapes changes only at these critical levels.

Thus, the flow complex filtration precisely captures the topological changes of the family of Čech complexes parametrized by α. Furthermore the definition of flow shapes has a strong Morse theoretic flavor which might allow the use of Morse theoretic concepts [72, 74, 102].

Example. For a set of balls (of radius $\sqrt{\alpha}$ for $\alpha > 0$) we obtain a sub-complex of the flow complex by only including the cells completely covered by the union of balls. The underlying space is called flow shape. In Section 6.4 we construct for all values of α a deformation retraction from the union of balls to the flow shape, i.e., the flow shape can be obtained by continuously shrinking the union of balls.

For an illustration consider Figure 6.1 which has the same input points as in the introduction of the previous chapter. It shows the filtration of the flow complex in comparison to the union of balls (see Figure 6.2 for a comparison of flow shapes to other shape constructors and Figure 6.3 for an example with points sampled from a surface). For $\alpha = 0$ the union of balls consists of the three input points. The flow shape is the underlying space of the cells corresponding to fixed points covered by the union of balls. Thus, for $\alpha = 0$ the flow shape also consists of the three input points and is equal to the union of balls. When α is increased, the balls grow but can be continuously shrunken back to the point set as long as none of the balls overlap (Figure 6.1(a)). In Figure 6.1(b) a pair of balls overlap. The area of overlap contains a fixed point of the flow and the corresponding cell has been added to the flow shape. The flow shape now consists of a line segment and a point. As before, the flow shape can be obtained by continuously shrinking the union of balls(but no longer only radially). Thus the flow shape and union of balls are again homotopy equivalent. When increasing α further, first the two other pairs of balls intersect and the corresponding line segments are added to the flow shape (Figure 6.1(c)). Eventually all three balls overlap and the cell constructed in the previous example

is added to the shape (Figure 6.1(d)).

To construct the deformation retraction, the algorithm for the flow complex can be used in the following way: Assume we have constructed the deformation retraction for Figure 6.1(c) and now want to construct it for Figure 6.1(d). In Figure 6.1(d) reducing α slightly (e.g. to the value of Figure 6.1(c)) will leave a small part of the flow shape uncovered. After removing this small part we can follow the steps of the algorithm to continuously shrink the corresponding cell of the flow complex to its boundary, and thus shrink the flow shape to the flow shape of Figure 6.1(c). Then, by again adding all parts removed we extend the deformation retraction of Figure 6.1(c) to Figure 6.1(d).

6.2 Preliminaries

We first introduce underlying concepts from topology and then the union of balls and the Čech complex.

Homotopy Equivalence and Deformation Retract. A *homotopy* is a continuous map $F : X \times [0,1] \to Y$. Two continuous maps $f_1, f_2 : X \to Y$ are *homotopic* (denoted by $f_1 \simeq f_2$), if there is a homotopy connecting them, i.e., $f_1(x) = F(x,0)$ and $f_2(x) = F(x,1)$.

A continuous map $f : X \to Y$ is called *homotopy equivalence* if there is a continuous map $g : Y \to X$ with $fg \simeq id_Y$ and $gf \simeq id_X$, where id_Y and id_X denote the identity map on Y and on X, respectively. In this case the spaces X and Y are said to be *homotopy equivalent* or to have the same *homotopy type*, denoted by $X \simeq Y$.

A homotopy $F : X \times [0,1] \to X$ is called *deformation retraction* of X to a subspace A if $F(x,0) = x$ for all $x \in X$, $F(X,1) = A$, and $F(a,t) = a$ for all $a \in A$ and $t \in [0,1]$. In this case $A \simeq X$ and A is called a *deformation retract* of X.

Mapping Cylinder Neighborhood. The following topological concepts are used in the proof of Theorem 6.6. For a more detailed and illustrated introduction to these concepts we refer to the textbook by Hatcher [77].

The *mapping cylinder* M_f of a continuous map $f : X \to Y$ is the quotient space of the disjoint union of $X \times [0,1]$ and Y formed by identifying $(x,0)$ of $X \times \{0\}$ with the point $f(x)$ in Y. A subspace A of X has a *mapping cylinder neighborhood* N in X if the neighborhood N contains a subspace B (considered as boundary of N) such that $N - B$ is an open neighborhood of A and there is a continuous map $f : B \to A$ and a homeomorphism $g : M_f \to N$ with

$$\begin{aligned} g(b,1) &= b \qquad \text{and} \\ g(b,0) &= f(b) \end{aligned}$$

for all $b \in B$.

We will use the following property of such a pair (X, A) (see [77], Example 0.15 and Corollary 0.20):

Proposition 6.1. *If A has a mapping cylinder neighborhood in X and the inclusion $A \hookrightarrow X$ is a homotopy equivalence, then A is a deformation retract of X.*

Union of Balls. For the power distance of a point p with positive weight w_p, $\sqrt{w_p}$ was interpreted as radius of a ball around p. Similarly, for a parameter α we will consider the *family of balls* $B_\alpha(P)$ with radii $\sqrt{\alpha + w_p}$ for all $p \in P$ with $\alpha + w_p \geq 0$. Thus with P_α defined as

$$P_\alpha := \{p \in P | \, \alpha + w_p \geq 0\}$$

the *union of balls* is the underlying space of $B_\alpha(P)$, i.e.,

$$|B_\alpha(P)| := \bigcup_{b \in B_\alpha(P)} b = \left\{ x \in \mathbb{R}^d \middle| \, \exists p \in P \text{ such that } \pi_p(x) \leq \alpha \right\}.$$

Čech Complex. The Čech complex $\check{\mathrm{C}}_\alpha(P)$ is the *nerve* [136] of the family of balls $B_\alpha(P)$, i.e., the simplicial complex with $B_\alpha(P)$ as vertex set and a simplex for every subset of balls with non-empty intersection. By the *nerve lemma* [91], the Čech Complex and the union of balls are homotopy equivalent.

The subcomplex obtained by restricting to the simplices for which the Voronoi cells corresponding to the balls share a (non-empty) face is the *α-shape complex*. It is a subcomplex of the Delaunay tessellation and is homotopy equivalent to the Čech Complex [58].

6.3 Flow Shapes

We have a natural filtration of the flow complex, i.e., a family of nested subcomplexes. By $F_\alpha(P)$ we denote the sub-complex of the flow complex that contains all stable manifolds of critical points at which the distance function h takes a value no more than α. The underlying space $|F_\alpha(P)|$ is called *flow shape*.

As discussed in Sections 5.1 and 6.2 further families of shapes and complexes are: The union of balls $|B_\alpha(P)|$, the Čech complex, and the α-shape complex. These families are parametrized by the distance level α and for a given distance level they are homotopy equivalent. In this section we prove that the flow shape $|F_\alpha(P)|$ is also homotopy equivalent to the union of balls. Before we proceed to the proof, we consider an example for these families.

Example. Figure 6.2 shows the union of balls, the Čech complex, the α-shape complex, and the flow shape on a set P of unweighted points in two dimensions. Three different values for α are shown in the three columns of the figure.

In the first row the union of balls is shown together with their Voronoi diagram. In the left figure α is small and the balls are still isolated. In the middle figure α is larger and some of the balls already overlap. In the right figure α is very large, such that all balls overlap.

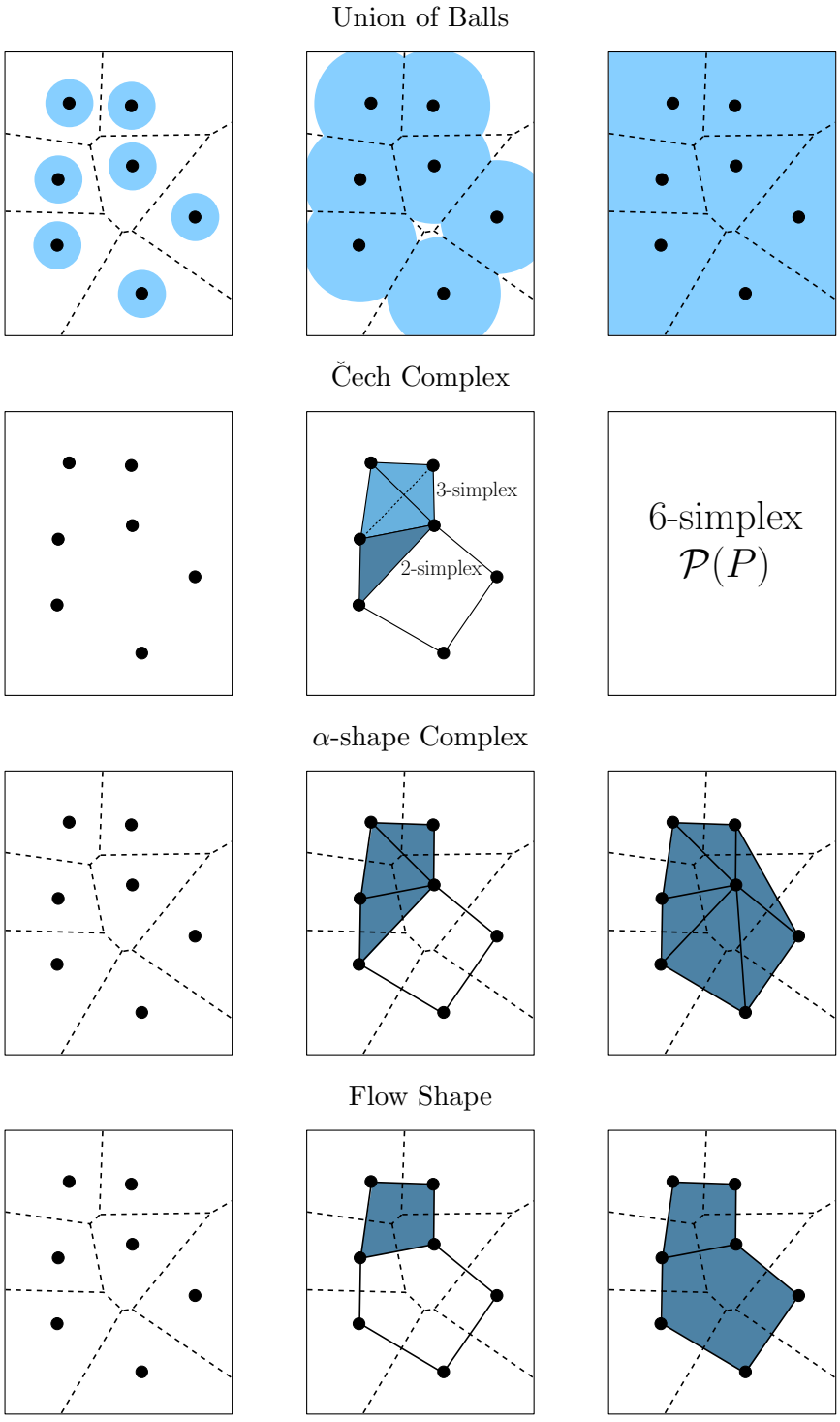

Figure 6.2: Example of parametrized shapes and complexes

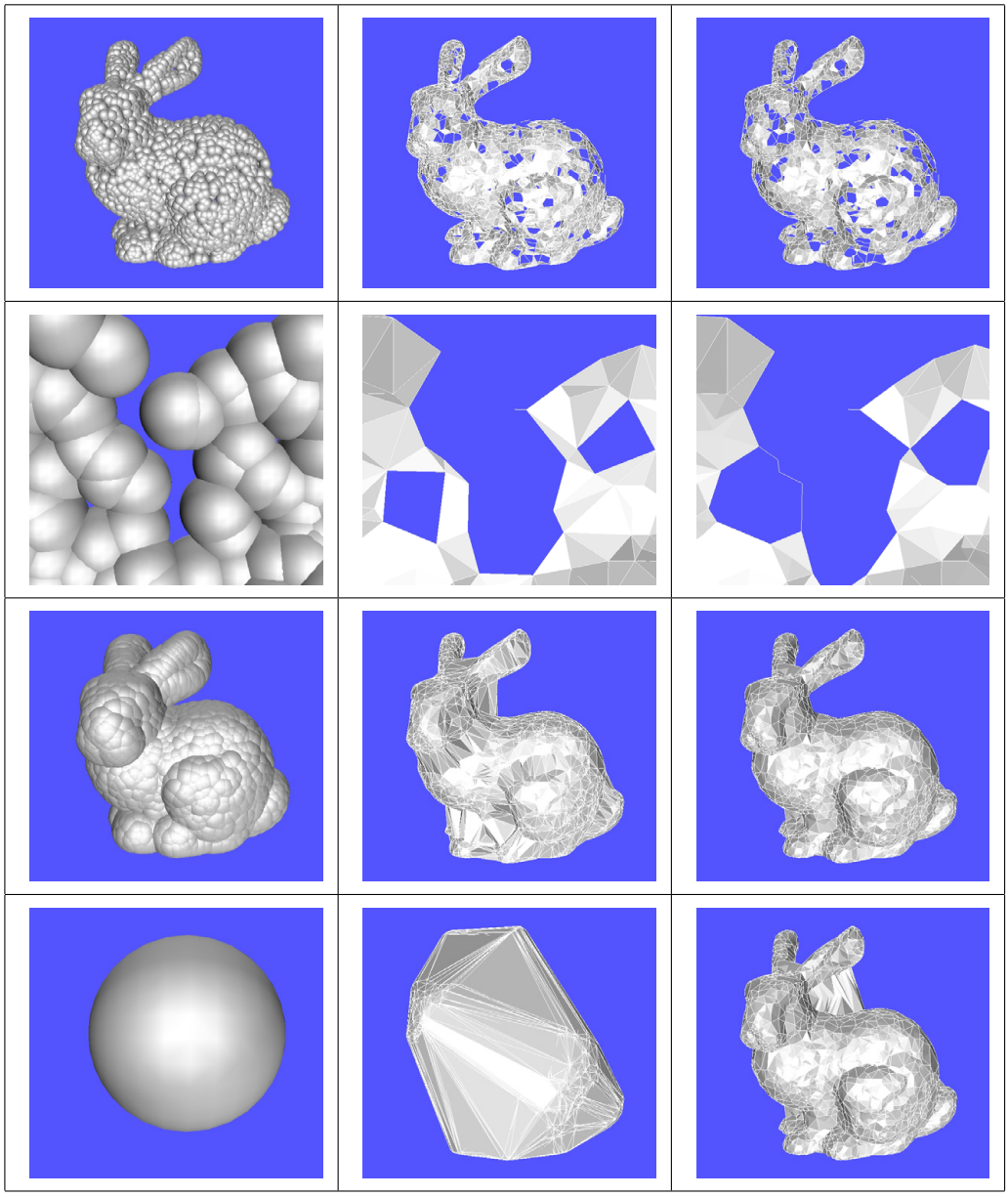

Figure 6.3: The union of balls (left), the α-shape (middle) and the flow shape (right) for increasing values of α (top to bottom). The second row shows a zoom of the pictures in the first row. The shapes in each row are homotopy equivalent.

The second row shows the Čech complex. It is an abstract simplicial complex, so the placement of the points does not indicate a position in the plane but are chosen as for the union of balls to identify the vertices. Since in the left row the balls are isolated, the complex consists only of the vertices. In the middle figure it consists of vertices, edges, triangles, and a tetrahedron. The tetrahedron is in the complex since the four corresponding balls have a common intersection. In the right figure, the complex is not depicted: all subsets of points form a simplex since their balls have a common intersection. Thus the complex is the power set $\mathcal{P}(P)$, i.e., a 6-dimensional simplex.

In the next row the α-shape complex is depicted. It contains only simplices for intersecting balls that also have a Voronoi face in common. For the isolated balls in the left row, the α-shape complex is again the set of points. In the middle figure it contains of the 3-simplex of the Čech complex only the two Delaunay triangles. In the right figure the α-shape complex equals the Delaunay tessellation of the points.

The bottom row shows the flow complex filtration. Again it starts with the set of points. In the middle figure several edges (stable manifolds of saddle points) and one two-dimensional face (the stable manifold of a maximum) are present. In contrast to the α-shape complex this face is not decomposed into two triangles, since it contains only one critical point. Also the further triangle which is present in the α-shape complex is not contained since it does not correspond to a critical point. In the right figure, one additional face is present, the stable manifold of the second local maximum. Further increase of α will not change the flow shape.

An example of flow shapes and other shape constructors on points sampled from a surface is shown in Figure 6.3. The figure illustrates that these shape constructors can be geometrically quite different although they are topologically equivalent. Note that the union of balls looks almost like a big ball at large levels. For the largest level a scaled version of the union of balls is shown.

6.4 Homotopy Equivalence of Union of Balls and Flow Shapes

We prove the homotopy equivalence of the union of balls and flow shape for a distance level α in several steps. First we will consider the levels α between two critical levels. In this case the homotopy type of both complexes does not change. Thus, we only need to consider critical levels. We separately consider how the union of balls and how the flow shape change at critical levels, and then combine this information to prove by induction over the critical values that the two complexes have the same homotopy type.

Between Critical Levels. By definition the flow shapes do not change between the critical values of the distance function. From the critical point theory of distance functions we get that an isotopy lemma as in Morse theory still holds (for the notions from Riemannian geometry see [121]).

Proposition 6.2 (Isotopy Lemma, Grove (Proposition 1.8) [74])**.** *Let M be a complete connected Riemannian manifold and $A \subset M$ a compact subset of M. Let $h_A \colon M \to \mathbb{R}$ denote the distance function of A. Suppose $[r_1, r_2] \subset \mathbb{R}_+$ contains only regular values for h_A. Then all the levels $h_A^{-1}(r)$, $r \in [r_1, r_2]$, are homeomorphic, and the annulus*

$$R(r_1, r_2) \;=\; D_A(r_2) - B_A(r_1) \;=\; \{\, q \in M \,|\, r_1 \leq h_A(q) \leq r_2 \}$$

is homeomorphic to $h_A^{-1}(r_1) \times [r_1, r_2]$.

We will mostly use the isotopy lemma in the following version, i.e., applied to the point set P and using only that the homotopy of the union of balls does not change between critical values. As in the previous chapter, we denote by h the distance function induced by the point set P, i.e.,

$$h(x) = \min \{\, \pi_p(x) \,|\, p \in P \}\,.$$

Corollary 6.3. *If the interval $[\alpha, \alpha'] \subset [0, \infty)$ does not contain any critical value of h, i.e., there is no critical point $x \in \mathbb{R}^d$ of h with $h(x) \in [\alpha, \alpha']$, then $|B_\alpha(P)|$ is homeomorphic to $|B_{\alpha'}(P)|$, and $|B_\alpha(P)|$ is a deformation retract of $|B_{\alpha'}(P)|$.*

Union of Balls at a Critical Level. The following lemma describes how the homotopy of the union of balls changes at critical values. The union of balls with parameter $\alpha + \varepsilon$ above a critical level α can be continuously deformed to the union of balls with parameter $\alpha - \varepsilon$ below the critical level with a small part of a Delaunay polytope glued in at each position of critical points at this level. We will use this later to glue in the same part into a flow shape.

Before proving Lemma 6.4 we illustrate the configuration at a critical point by the example of Figure 6.4. It shows a critical point c defined by the two points p and p'. The distance level of c is α, i.e., both the distance from p to c and from p' to c is $\sqrt{\alpha}$. Therefore the unions of balls $|B_{\alpha-\varepsilon}| = b_{\alpha-\varepsilon} \cup b'_{\alpha-\varepsilon}$ and $|B_{\alpha+\varepsilon}| = b_{\alpha+\varepsilon} \cup b'_{\alpha+\varepsilon}$ are not homotopy equivalent. The points p and p' define a Delaunay face D. The part of D that we add to the smaller union of balls is $D_\varepsilon := D \setminus B_{\alpha-\varepsilon}$.

Now $|B_{\alpha+\varepsilon}|$ can be shrunk to $|B_{\alpha-\varepsilon}| \cup D_\varepsilon$ in the following way. In the proximity of a critical point an orthogonal shrinking is chosen as indicated by the two black arrows in the figure. Outside of the proximity of any critical point a radial shrinking is chosen as indicated by the gray arrows.

The different types of shrinking can be combined by a partition of unity. But instead of constructing the shrinking explicitly we will again apply the critical point theory for distance functions, i.e., Proposition 6.2. If the direction of the arrows in Figure 6.4 is reverted, they indicate a set of generalized gradients for $|B_{\alpha-\varepsilon}| \cup D_\varepsilon$. The following lemma generalizes an observation by Siersma [134] for the union of disks in two dimensions (cf. also Lemma 1.13 in [74]).

Lemma 6.4. *Let α be a critical value of the distance function and $c_1, \ldots, c_m$ with $m \geq 1$ the critical points at value α. Let V_i be the lowest dimensional Voronoi face containing c_i and D_i the dual Delaunay face for $1 \leq i \leq m$.*

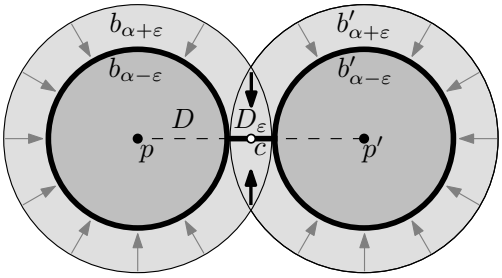

Figure 6.4: The set $b_{\alpha-\varepsilon} \cup b'_{\alpha-\varepsilon} \cup D_\varepsilon$ is a deformation retract of $b_{\alpha+\varepsilon} \cup b'_{\alpha+\varepsilon}$.

There is an $\varepsilon > 0$ such that $D_{i,\varepsilon} := D_i \setminus |B_{\alpha-\varepsilon}|$ is a topological ball (of the same dimension as D_i) containing c_i for $1 \leq i \leq m$, and $|B_{\alpha-\varepsilon}| \cup D_{1,\varepsilon} \cup \ldots \cup D_{m,\varepsilon}$ is a deformation retract of $|B_{\alpha+\varepsilon}|$.

Proof. We first restrict our attention to the case of one critical point c. Then we generalize the argument to a set of critical points.

Let V the lowest dimensional Voronoi face containing the critical point c, D the dual Delaunay face, and $D_\varepsilon := D \setminus |B_{\alpha-\varepsilon}|$ (as in Figure 6.4). Since c is a critical point and therefore its own driver, c is contained in D_ε.

Let U be the union of the Voronoi cells of the vertices of D. Since $c \in V^\circ$ and $V \subset U$, a neighborhood of c is contained in U°. Let $\varepsilon > 0$ be chosen such that the interval $[\alpha - \varepsilon, \alpha + \varepsilon]$ contains no critical value except α and that a $\sqrt{2\varepsilon}$-neighborhood of D_ε is contained in U°.

Instead of applying Proposition 6.2 to the point set P we apply it to the compact set K with

$$K := P \cup D_\varepsilon.$$

The weight of all points in D_ε is set to $\varepsilon - \alpha$. This gives that the points with distance at most $\alpha - \varepsilon$ to K are the points with distance at most $\alpha - \varepsilon$ to P and the points on D_ε. E.g., in Figure 6.4 the set of these points is the union of $b_{\alpha-\varepsilon}$, $b'_{\alpha-\varepsilon}$, and D_ε.

We prove that the levels α' with

$$\alpha - \varepsilon < \alpha' \leq \alpha + \varepsilon$$

are regular for the distance function h_K of K.

At the distance level $\alpha + \varepsilon$ the influence of D_ε is limited to a $\sqrt{2\varepsilon}$-neighborhood of D_ε and therefore by construction limited to U°. Points outside of this neighborhood in $|B_{\alpha+\varepsilon}| \setminus |B_{\alpha-\varepsilon}|$ are regular for h_K.

For a point $x \in U^\circ \setminus \mathit{aff}(D)$ let $N_K(x)$ denote the set of closest points in K to x. Since $N_K(x)$ is contained in D, the vector pointing orthogonally away from $\mathit{aff}(D)$ forms an angle less than $\pi/2$ with the vectors from the points in $N_K(x)$ to c. Thus, this vector is a generalized gradient at x (even though it is not necessarily a gradient) and x is a regular point of h_K (see Section 5.3.1).

By Proposition 6.2 this gives that the level sets $h_K^{-1}(\alpha')$ are homeomorphic, and $|B_{\alpha+\varepsilon}|$ can be deformation retracted to K. For the above argument, only the generalized gradients in a small neighborhood of c had to be considered.

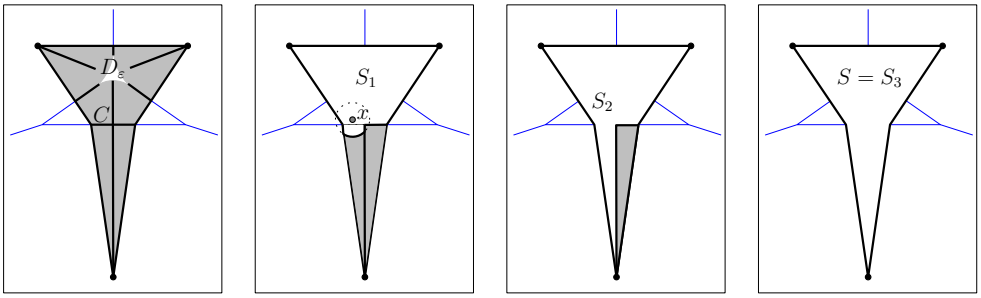

Figure 6.5: Steps in the deformation retract in the proof of Lemma 6.5.

If we define $K' := P \cup D_{1,\varepsilon} \cup \ldots \cup D_{m,\varepsilon}$ and consider h'_K the argumentation directly generalizes to a set of critical points by choosing $\varepsilon > 0$ in such a way that the $\sqrt{2\varepsilon}$-neighborhoods of the $D_{i,\varepsilon}$ $(i = 1, \ldots m)$ do not overlap. □

Flow Shape at a Critical Level. For the union of balls we can describe the change of topology at a critical level by gluing in neighborhoods of the critical points. We have an analogous result for flow shapes: By taking out small neighborhoods out of the shape at the critical level, we can retract it to the shape of the previous critical level.

Lemma 6.5. *Let α be a critical value of the distance function and $c_1, \ldots, c_m$ with $m \geq 1$ the critical points at value α. Let V_i be the lowest dimensional Voronoi face containing c_i and D_i the dual Delaunay face for $1 \leq i \leq m$.*

There is an $\varepsilon > 0$ such that $|F_{\alpha-\varepsilon}|$ is a deformation retract of $|F_\alpha| \setminus (D_{1,\varepsilon} \cup \ldots \cup D_{m,\varepsilon})$ where $D_{i,\varepsilon} := D_i \setminus |B_{\alpha-\varepsilon}|$ for $1 \leq i \leq m$.

Proof. We present a deformation retract using the structure of stable manifolds inherently described by the algorithm Inflow. We retract maximal polytopal faces of a stable manifold S one at a time such that $\overline{S} \setminus D_\varepsilon$ is retracted to the faces it shares with the closures of stable manifolds S' with $S' < S$. By Lemma 5.11 these stable manifolds are present in $|F_\alpha|$. For the deformation retraction it is necessary that co-faces of the polytopal faces of S that we want to retract are not yet present in the restricted flow complex. This is guaranteed by Lemma 5.11. In particular, the stable manifolds of the same critical level do not influence each other. We can therefore restrict the analysis to the case of one critical point at the critical level α. In the case of several critical points we can retract them one at a time.

Let $\varepsilon > 0$ be chosen such that the interval $[\alpha - \varepsilon, \alpha + \varepsilon]$ contains no critical value except α. Let c be the critical point at level α, S its stable manifold, V the lowest dimensional Voronoi face containing c, D the dual Delaunay face, and $D_\varepsilon := D \setminus |B_{\alpha-\varepsilon}|$.

The steps of the deformation retract are illustrated in Figure 6.5 by the example of the weighted two-dimensional point set previously used. In the example we want to retract the stable manifold corresponding to the two-dimensional part of the flow complex. In Figure 6.5(a)-(d) always the parts that have been

already retracted are labeled while the remaining part is shown shaded in gray. Figure 6.5(a) shows the stable manifold with D_ε removed.

The algorithm INFLOW successively processes a sequence of Voronoi faces (its second argument). For the proof we rearrange the order of processing these Voronoi faces in a breadth first manner: we collect all flow from higher dimensional Voronoi faces before we collect flow from the boundary of a Voronoi face. For the implementation this means that instead of using a stack as it is implicitly done with the recursive calls, we use a queue. We first gather all cells intersected by D_ε and retract to the boundary of the corresponding inflow region. From there, we retract cell by cell.

This gives a sequence of cells as follows: we start with a point (the critical point) and a Voronoi face V that contains the point. Then we process all Voronoi faces that contain V. Whenever we process new flow coming from the boundaries of previously processed Voronoi cells a new step in the sequence starts. Assume that we have N steps in the sequence and let $S_j, j = 1, \ldots, N$, be the interior of the part of the stable manifold S of c that has been constructed after finishing step j of the sequence. In the example of Figure 6.5 we have three parts of the stable manifold S in the sequence: S_1 is the part reached without crossing the boundary of a Voronoi cell. Then S_2 additionally includes the lower left triangle of the remaining part and $S_3 = S$ the right triangle.

We show by induction over N that $\overline{S} \setminus D_\varepsilon$ deformation retracts to $\overline{S} \setminus S_N = \overline{S} \setminus S = \partial S$. Note that deformation retracts are transitive in the sense that if X_1 is a deformation retract of X_2, and X_2 is a deformation retract of X_3 then X_1 is a deformation retract of X_3.

We first show that $\overline{S} \setminus D_\varepsilon \simeq \overline{S} \setminus S_1$ holds by a deformation retract. For this consider the boundary ∂S_1 of S_1. It has the structure of a polyhedral complex and is visible from the critical point. With D_ε removed we can therefore retract (radially from c) to the boundary of S_1. For the induction step we construct a deformation retract from $\overline{S} \setminus S_j$ to $\overline{S} \setminus S_{j+1}$ for $1 \leq j < N$. For this we consider a cell C of $\partial S_j \cap S_{j+1}$ together with the corresponding Voronoi face V. We proceed by showing that the area of flow onto C from higher-dimensional Voronoi faces can be retraced starting at C. We cannot directly follow the direction of flow since the resulting map would not be continuous at the boundary. Instead we use the following retraction: we choose a point x that is outside of C' and that sees all interior points of C' through the interior of C, i.e., the line through x and any point in the interior of C' intersects C. Such a point exists (close to C) since C' is a convex polytope with C as a facet. Now C' can be retracted starting at C radially away from x until a boundary of C' (other than C) is hit. This process is shown in Figure 6.5(b) for the case $j = 1$. In the figure, S_1 has been already removed and C has been radially pushed away from x.

Lower dimensional parts of S_j might remain which we can retract in the same way. In the example of the figure this is not necessary for S_2, but in the next step, i.e., when the right triangle is retracted, the middle segment remains which then is retracted. From this we get a deformation retraction from $\overline{S} \setminus S_j$ to $\overline{S} \setminus S_{j+1}$ for $1 \leq j < N$, and by induction a deformation retraction from $\overline{S} \setminus D_\varepsilon$ to $\overline{S} \setminus S_N = \partial S$. Figure 6.5(d) shows the situation where all of $S = S_3$ has been retracted to its boundary. □

Homotopy Equivalence. We are now prepared to prove the main theorem of this section.

Theorem 6.6. *Let P be a finite set of weighted points in $\mathbb{R}^d$. For every $\alpha \geq 0$ the flow shape $|F_\alpha(P)|$ is homotopy equivalent to the union of balls $|B_\alpha(P)|$.*

Proof. The homotopy type of both $|B_\alpha(P)|$ and $|F_\alpha(P)|$ changes only at critical values of the distance function h, and $|F_\alpha(P)|$ only changes at these levels at all. For levels α, α' between two critical levels $|B_\alpha(P)|$ is a deformation retract of $|B'_\alpha(P)|$ by Corollary 6.3.

Thus, it suffices to check that $|F_\alpha(P)|$ stays homotopy equivalent to $|B_\alpha(P)|$ if α passes a critical level.

We prove by induction that for all critical values α, $|F_\alpha(P)|$ is a deformation retract of $|B_{\alpha+\varepsilon}(P)|$ for a suitable $\varepsilon > 0$.

Without loss of generality we assume that all points have non-positive weights and the largest weight is 0. This can be achieved by subtracting the largest weight from all others. Thus, h is positive and 0 is the smallest critical value.

Let $0 = \alpha_0 < \alpha_1 < \cdots < \alpha_n$ be the critical values of h. Note that there can be only finitely many critical points of h by Lemma 5.3. Assume that $|F_\alpha(P)|$ is a deformation retract of $|B_\alpha(P)|$ for all $\alpha \leq \alpha_{i-1} + \varepsilon$, where $\varepsilon > 0$ is chosen such that it satisfies the following:

(i) The ε-neighborhood of any critical value α_j $(0 \leq j \leq n)$ does not contain any other critical value.

(ii) $0 < \varepsilon < \min\{\varepsilon_c | \, c \text{ a critical point}\}$, where $\varepsilon_c > 0$ is chosen such that $D_{i,\varepsilon_c} \subset S$, where D_{i,ε_c} is defined as before (see Lemma 6.4). The existence of such an ε_c follows from the recursive construction of the stable manifold S of c in the algorithm Inflow.

For $\alpha_0 = 0$ we have $|B_{\alpha_0}(P)| = P_0 = |F_{\alpha_0}(P)|$, where P_0 is the set of points of weight 0. By retracting balls to points, we get that $|F_{\alpha_0}(P)|$ is a deformation retract of $B_{\alpha_0+\varepsilon}$.

In the induction step, we need to prove that $|F_{\alpha_i}(P)|$ is a deformation retract of $|B_{\alpha_i+\varepsilon}(P)|$. By the induction hypothesis we have that $|F_{\alpha_{i-1}}(P)|$ is a deformation retract of $|B_{\alpha_{i-1}+\varepsilon}(P)|$. By Corollary 6.3 we have for all $\alpha_{i-1}+\varepsilon \leq \alpha' < \alpha_i$ that $|B_{\alpha_{i-1}+\varepsilon}(P)|$ is a deformation retract of $|B_{\alpha'}(P)|$. Thus $|F_{\alpha'}(P)| = |F_{\alpha_{i-1}}(P)|$ is a deformation retract of $|B_{\alpha'}(P)|$.

Let $c_1, \ldots, c_m$ be the critical points of h at α_i and $D_{1,\varepsilon}, \ldots D_{m,\varepsilon}$ defined as before (see Lemma 6.4).

We construct the deformation retraction in two steps: In the first step we prove that

$$A \quad := \quad |F_{\alpha_i}(P)| \setminus (D_{1,\varepsilon} \cup \ldots \cup D_{m,\varepsilon})$$

is a deformation retract of

$$X \quad := \quad |B_{\alpha_i-\varepsilon}(P)|.$$

In the second step we extend this to a deformation retraction from $|F_{\alpha_i}(P)|$ to $|B_{\alpha_i+\varepsilon}(P)|$.

For the first step we use Proposition 6.1. We have $A \subset X$. Let N be an ε'-neighborhood of A in X for a sufficiently small $\varepsilon' > 0$, i.e., such that the distance function of A has no critical value in the interval $[0, \varepsilon']$. Proposition 6.2 applied to A yields that N is a mapping cylinder neighborhood of A.

Next, we need to prove that the inclusion $\iota : A \hookrightarrow X$ is a homotopy equivalence. Thus we need a map $g : X \to A$ such that

$$\iota \circ g \simeq id_X \qquad \text{and} \qquad g \circ \iota \simeq id_A.$$

Let $G : X \times [0,1] \to X$ be the deformation retraction of X to $|F_{\alpha_{i-1}}(P)|$ given by the induction hypothesis. Let $g : X \to A$ be defined by $g(x) = G(x, 1)$. The map $\iota \circ g$ is simply $G(\cdot, 1) : X \to X$ and therefore by induction hypothesis homotopic to id_X.

The map $g \circ \iota$ is the restriction of g to A and therefore maps A to $|F_{\alpha_{i-1}}(P)|$. By Lemma 6.5, $|F_{\alpha_{i-1}}(P)|$ is a deformation retract of A, thus the map $g \circ \iota$ is homotopic to id_A.

By Proposition 6.1, A is a deformation retract of X. The retract is constant on

$$\partial D_{1,\varepsilon} \cup \ldots \cup \partial D_{m,\varepsilon}$$

since this union is in A. We can extend the deformation retraction by the identity map on $D_{1,\varepsilon} \cup \ldots \cup D_{m,\varepsilon}$ to a deformation retraction from

$$X' \quad := \quad |B_{\alpha_i - \varepsilon}(P)| \cup D_{1,\varepsilon} \cup \ldots \cup D_{m,\varepsilon} \quad = \quad X \cup D_{1,\varepsilon} \cup \ldots \cup D_{m,\varepsilon}$$

to

$$A' \quad := \quad |F_{\alpha_i}(P)| \quad = \quad A \cup D_{1,\varepsilon} \cup \ldots \cup D_{m,\varepsilon}.$$

By Lemma 6.4, X' is a deformation retract of $|B_{\alpha_i + \varepsilon}|$. This concludes the induction. We have proved that between any two critical levels the homotopy type of the flow shape and the union of balls are the same. Since the homotopy type only changes at critical levels, it also has to be the same at the critical levels. We therefore have for all levels α of the distance function h that $|F_\alpha(P)| \simeq |B_\alpha(P)|$. □

Conclusion

We proved that the unions of balls and flow shapes are homotopy equivalent based on the recursive geometry of the flow complex. This places flow shapes in a class of topologically equivalent shape constructors. In their geometry these shape constructors can be quite different as was illustrated using Figure 6.3 by a comparison to α-shapes.